Neomycin B−Arginine Conjugate, a Novel HIV-1 Tat Antagonist: Synthesis and Anti-HIV Activities†

Alexander Litovchick,‡,§ Aviva Lapidot,*,‡ Miriam Eisenstein,|| Alexander Kalinkovich,⊥ and Gadi Borkow⊥

Department of Organic Chemistry, Weizmann Institute of Science, 76100 Rehovot, Israel, Unit of Chemical Services, Weizmann Institute of Science, 76100 Rehovot, Israel, and Ruth Ben-Ari Institute of Clinical Immunology and AIDS Center, Kaplan Medical Center, Hebrew University Hadassah Medical School, 76100 Rehovot, Israel

Received April 27, 2001; Revised Manuscript Received September 5, 2001

ABSTRACT: HIV-1 transactivating protein Tat is essential for virus replication and progression of HIV disease. HIV-1 Tat stimulates transactivation by binding to HIV-1 transactivator responsive element (TAR) RNA, and while secreted extracellularly, it acts as an immunosuppressor, an activator of quiescent T-cells for productive HIV-1 infection, and by binding to CXC chemokine receptor type 4 (CXCR4) as a chemokine analogue. Here we present a novel HIV-1 Tat antagonist, a neomycin B−hexaarginine conjugate (NeoR), which inhibits Tat transactivation and antagonizes Tat extracellular activities, such as increased viral production, induction of CXCR4 expression, suppression of CD3-activated proliferation of lymphocytes, and upregulation of the CD8 receptor. Moreover, Tat inhibits binding of fluoresceine isothiocyanate (FITC)-labeled NeoR to human peripheral blood mononuclear cells (PBMC), indicating that Tat and NeoR bind to the same cellular target. This is further substantiated by the finding that NeoR competes with the binding of monoclonal Abs to CXCR4. Furthermore, NeoR suppresses HIV-1 binding to cells. Importantly, NeoR accumulates in the cell nuclei and inhibits the replication of M- and T-tropic HIV-1 laboratory isolates ($EC_{50} = 0.8-5.3\ \mu M$). A putative model structure for the TAR−NeoR complex, which complies with available experimental data, is presented. We conclude that NeoR is a multitarget HIV-1 inhibitor; the structure, and molecular modeling and dynamics, suggest its binding to TAR RNA. NeoR inhibits HIV-1 binding to cells, partially by blocking the CXCR4 HIV-1 coreceptor, and it antagonizes Tat functions. NeoR is therefore an attractive lead compound, capable of interfering with different stages of HIV infection and AIDS pathogenesis.

The development of novel human immunodeficiency virus type 1 (HIV-1)[1] inhibitors, targeted against viral components other than HIV reverse transcriptase (RT) or protease, is of special importance in view of the failure, in many cases, of the current antiretroviral therapies, and due to the emerging and high variability of resistant HIV-1 strains. A current direction in this field is the development of HIV transcription transactivator protein (Tat) inhibitors, which may be critical for anti-AIDS strategies due to the multiplicity and diversity of Tat functions in the HIV life cycle and AIDS pathogenesis (*1*−*4*). Tat is a small (14 kDa) multifunctional viral regulatory protein. Its primary function is the transactivation of the transcription from HIV long terminal repeats (reviewed in refs *5* and *6*). However, Tat functions not solely as an HIV gene regulator; while secreted extracellularly, it also acts as an immunosuppressor, an activator of quiescent T-cells for productive HIV-1 infection, a chemokine analogue, and an apoptosis inducer (*2*, *4*, *7*−*9*). Tat also induces peripheral blood mononucleated cell apoptosis (*10*, *11*), probably contributing to CD4+ T-cell depletion, characteristic of AIDS. In addition, extracellular Tat upregulates

† The work was supported in part by research grants from the Israeli Ministry of Sciences, Yeda Research Co. (WIS), internal grants of the Weizmann Institute to A. Lapidot, and grants from The Institute of Advanced Therapy (IAT) for the Center of Excellence in AIDS Research in Israel, and the Horowitz Foundation, granted to the Kaplan AIDS Center.

* To whom correspondence should be addressed: Department of Organic Chemistry, Weizmann Institute of Science, 76100 Rehovot, Israel. Telephone: 972-8-934 3413. Fax: 972-8-934 4142 or 972-8-934 2559. E-mail: aviva.lapidot@weizmann.ac.il.

‡ Department of Organic Chemistry, Weizmann Institute of Science.

§ Current address: Department of Biological Chemistry and Molecular Pharmacology, Harvard Medical School, 250 Longwood Ave., Boston, MA 02115.

|| Unit of Chemical Services, Weizmann Institute of Science.

⊥ Kaplan Medical Center.

[1] Abbreviations: AAC, aminoglycoside−arginine conjugates; R3G, triarginine−gentamicin C conjugate; R4K, tetraarginine−kanamycin conjugate; GB4H, tetra-γ-guanidinobutyric acid−kanamycin conjugate; NeoR, hexaarginine−neomycin B conjugate; Tat, transactivator of transcription; TAR, transactivator responsive element; CXCR4, CXC chemokine receptor type 4; CCR5, CC chemokine receptor type 5; EC_{50}, 50% effective concentration; CC_{50}, 50% cytotoxic concentration; IC_{50}, 50% inhibitory concentration; TI_{50}, 50% in vitro therapeutic index; K_d, constant for dissociation of RNA and a fluorescently labeled tracer (RevRh); K_D, constant for dissociation of RNA and a competitor to the labeled tracer (RevRh); HIV-1, human immunodeficiency virus type 1; CD3, T-cell receptor; CD8, receptor of the main histocompatibility complex molecule, type I; CD4, receptor of the main histocompatibility complex molecule, type II; HPLC, high-performance liquid chromatography; MTT assay, tetrazolium-based colorimetric assay; TCA, trichloroacetic acid; PBMC, peripheral blood mononuclear cells; FCS, fetal calf serum; PHA, phytohemagglutinin; IL, interleukin; PBS, phosphate-buffered saline; AZT, 3′-azido-3′-deoxythymidine, zidovudine; 3TC, 2′,3′-dideoxy-3′-thiacytidine, lamivudine; PE, phycoerithrine; FITC, fluorescein isothiocyanate; NMR, nuclear magnetic resonance; RT, reverse transcriptase; ERT, endogenous reverse transcription; mAb, monoclonal antibody; SDF-1α, stromal cell-derived factor 1α.

10.1021/bi0108655 CCC: $20.00 © 2001 American Chemical Society
Published on Web 12/01/2001

expression of chemokine receptors on lymphocytes, including the expression of CXCR4 and CCR5 (*12*−*14*), which serve as HIV-1 entry coreceptors, and enhances angiogenesis, inducing Kaposi's sarcoma, an angioproliferative disease, very frequent and aggressive in association with AIDS (reviewed in ref *3*).

These diverse functions of Tat are mainly provided by the cysteine rich domain (amino acids 21−40) (*15*) and the basic domain of the protein (amino acids 49−57) constituted by a stretch of repeated Arg and Lys residues (*16*−*18*). These domains, which are well-conserved among Tat proteins isolated from different strains of HIV-1 (*15*−*17*), are necessary for Tat stability (*19*) and interaction with nucleic acids (*20*). Moreover, peptides representing these domains are able to enhance transactivation, induce HIV replication, and trigger extracellular related Tat activities (reviewed in ref *6*).

The site of binding of Tat protein on TAR RNA is comprised of the UCU bulge and base pairs at both sides of it (*21*, *22*). Tat interaction with TAR is mediated by a nine-amino acid region (RKKRRQRRR, residues 49−57) of the protein. Tat-derived basic peptides (*23*) and even a nona-arginine peptide (*21*) bind TAR RNA with high affinity in vitro. Much less efficient than peptides is the aminoglycoside antibiotic neomycin B that binds to TAR RNA at the lower stem and the uridine rich bulge region (*24*, *25*), which adopts a conformation different from that known for TAR−Tat interactions (*26*, *27*).

The development of Tat protein inhibitors and antagonists comprises an important direction in anti-AIDS drug discovery. On the basis of peptide models of TAR RNA binding, NMR structures of TAR−ligand complexes, and aminoglycoside−RNA interactions, we designed and synthesized a novel HIV-1 Tat antagonist, a neomycin B−arginine conjugate (NeoR), and tested its activities against HIV-1 Tat. This aminoglycoside−arginine conjugate displays high affinity for TAR RNA in vitro, readily penetrates cells, and inhibits Tat transactivation in cell culture. It also antagonizes Tat extracellular activities, such as increased viral production, upregulation of CXCR4 HIV-1 coreceptor expression, suppression of CD3-activated proliferation of lymphocytes, and upregulation of the CD8 receptor. In addition, NeoR inhibits HIV-1 infection, partially by interacting with CXCR4 and blocking HIV-1 binding to cells, making NeoR a highly attractive HIV inhibitor.

Preliminary attempts to study the structure of a complex formed between TAR RNA and aminoglycoside−arginine conjugates experimentally (e.g., by NMR, or crystallization of such complexes) suggested that there is considerable flexibility in these complexes. Therefore, we undertook a theoretical study to predict the modes of interaction between TAR and NeoR. We examined whether one or more binding modes exist, and generated a putative model structure for the TAR−NeoR complex, which conforms to the available experimental data.

EXPERIMENTAL PROCEDURES

Synthesis and Characterization of the Hexaarginine−Neomycin B Conjugate (NeoR). NeoR (Figure 1) was synthesized as follows. Approximately 5 mmol of a water solution of free base aminoglycoside and neomycin B (Fluka, Rehovot, Israel) was used for the preparation of NeoR. For each amino group of the aminoglycoside, 1.1 equiv of N_{α}-carbobenzoxy-N_{ω}-nitroarginine (Sigma, Rehovot, Israel), dissolved in 40 mL of an ethanol/dioxane/water (1:1.5:0.5) mixture, and 1.2 equiv of a dry powder of 1-[3-(dimethylamino)propyl]-3-ethylcarbodiimide hydrochloride (Aldrich, Rehovot, Israel) were added to the aminoglycoside solution in 8−12 portions over the course of 24 h. The reaction was allowed to proceed for an additional 24−36 h at room temperature. The reaction progress was monitored by analytic thin-layer chromatography on silica gel plates in a chloroform/methanol/water running buffer (1:1:0.3). After completion of the reaction, the solvents were evaporated in vacuo, the residue was then extracted subsequently with deionized water, with 100 mM NaOH, and again with deionized water. The residue was dissolved in alcohol (75−80%) at 45 °C. The protected conjugate was precipitated with an equal volume of diethyl ether at 4 °C. The residue was dissolved in an alcohol/dioxane/water (1:1:1) mixture containing 1−1.5 equiv of acetic acid per each protected charged group (based on theoretical yield), and hydrogenated at atmospheric pressure for 12−20 h over 0.5 g of 10% Pd/charcoal catalyst. After this treatment, the solvents were evaporated in vacuo and the residue was dissolved in water (or a water/alcohol mixture), a fresh portion of acetic acid was added, and the hydrogenation was continued for an additional 24 h. The catalyst was removed by centrifugation, and the solution was evaporated in vacuo, which was then dissolved in water (NeoR acetate). The NeoR acetate salt was precipitated with alcohol. The precipitate was collected by centrifugation, washed with ether, and dried, which resulted in a hygroscopic white powder of NeoR acetate salt (overall yield of ∼30%). The compound was characterized by ^{1}H and ^{13}C NMR (see Results) and HPLC, using a YMC AQ C18 column (pore size of 200 Å) in a 25 min gradient from 0 to 50% acetonitrile and water at a rate of 0.5 mL/min. Peaks of interest, which eluted at 13.4 min, correspond to the hexaarginine−neomycin B conjugate as the main peak (∼90% of the total peak areas), and several small peaks probably arise from different degrees of arginine substitution (Figure 1 of the Supporting Information). The main HPLC peak was collected and further identified by mass spectroscopy (MALDITOF).

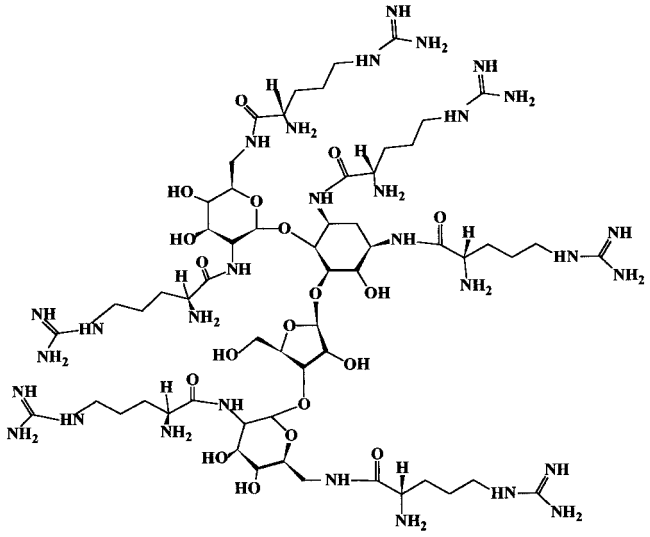

FIGURE 1: Structure of the neomycin B−hexaarginine conjugate.

Gel Shift RNA Binding Assay. Binding of NeoR to HIV-1 TAR RNA was examined by gel shift analysis basically as described previously (*28*, *29*). Briefly, a 31-residue TAR RNA fragment (5′-GGC CAG AUC UGA GCC UGG GAG CUC UCU GGC C-3′), containing residues 18−44 of HIV-1 LTR, synthesized by Dharmacon Research, Inc. (Boulder, CO), was ^{32}P-5′-end-labeled with T4 polynucleotide kinase (Promega, Madison, WI). The binding reaction mixtures (20 μL), containing 12 nM [^{32}P]TAR RNA and NeoR in 10 mM Tris-HCl (pH 7.5), 70 mM NaCl, 0.2 mM EDTA, and 5% glycerol, were incubated for 10 min on ice and resolved by electrophoresis on a 10% nondenaturing polyacrylamide gel (40:1 acrylamide:bisacrylamide). For comparison, we used the model Tat HIV peptide [Tat R52 (YKKKRKKKKKA)] as described previously (*21*). Quantitations were obtained by optical densitometry of the gels. Different concentrations of TAR RNA (6, 12, and 20 nM) were titrated with various concentrations of the Tat model peptide (R52) in the binding reactions. CD_{50} values are defined as the concentrations of NeoR or Tat R52 that produced 50% binding to TAR RNA.

Fluorescence Anisotropy Measurement of the Level of RNA Binding. Rhodamine-Rev peptide (residues 34−50, TRQARRNRRRRWRERQR) (RevRh) was prepared as previously described (*30*), and used as a fluorescence probe for binding to the 31-mer TAR RNA (described above). The rhodamine moiety is attached to the peptide N-terminus via an amide bond. The TAR RNA was annealed by heating to 95 °C with gradual cooling to room temperature. All stock solutions were prepared in nuclease free water and were diluted with appropriate buffers prior to use. RNA concentrations were determined spectrophotometrically at 260 nm, and the samples were re-annealed each time.

Binding of RevRh to HIV TAR RNA and NeoR competition with RevRh on binding to TAR RNA were examined with a fluorescence anisotropy assay (*30*, *31*). Fluorescence anisotropy measurements were performed on an SLM-Aminco model 8100 Series 2 spectrometer (Spectronic Instruments) equipped with a thermostat accurate to ±0.1 °C. The TAR binding samples (0−200 nM) were excited at 550 nm and monitored at 580 nm; the integration time was 4 s. Every point consists of 10−20 measurements, and their average values were used for calculation. Measurements were performed at 20 °C in a buffer solution containing 140 mM NaCl, 5 mM KCl, 1 mM $MgCl_2$, 1 mM $CaCl_2$, and 20 mM HEPES [4-(2-hydroxyethyl)-1-piperazineethanesulfonic acid] (pH 7.5) (*30*). The RevRh tracer concentration (0−70 nM) was determined spectroscopically at 550 nm. Different NeoR concentrations (0−140 nM in 20 nM lots) were used for the competition studies. The dissociation constants (K_d) for the RNA and fluorescently labeled tracer (RevRh), and the dissociation constant (K_D) of the RNA and the competitor (in our case, NeoR), were determined by nonlinear curve fitting, using the equations described previously (*30*, *31*), and are presented as mean values of three independent measurements (Figure 2 of the Supporting Information).

Cellular Uptake Using a Fluorescent Probe (NeoR−FITC). The fluorescent derivative of NeoR was prepared by reacting NeoR with fluorescein isothiocyanate (FITC, Sigma) in a 1:1 molar ratio, in a water/methanol/dioxane (1:1:1, v/v) mixture for 1 h at room temperature. After removal of the solvents (under reduced pressure), the NeoR−FITC conjugate was purified by extraction with absolute ethanol. The FITC conjugate was finally dissolved in water. The FITC conjugation is via the *N*-α-amino group of the arginine. Human peripheral blood mononuclear cells (PBMC), separated from a fresh blood sample on a Ficoll gradient by the standard procedure and hippocampal neurons from rat puppies, were cultured on polylysine-coated glass cover slides (*28*). The cells were incubated with the NeoR−FITC conjugate in HEPES-buffered saline for 30 min. The slides were washed several times with a saline solution and studied by confocal laser-scanning microscopy on an Axiovert 100M (Zeiss) microscope, using excitation at 488 nm (argon ion laser) and emission detected in a band of 505−550 nm.

HIV-1 Isolates and Cell Culture. PBMC, MT2, cMAGI, and U937 cell lines, and H9+ cells chronically infected with HIV-1 III_B, were cultured in RPMI 1640 medium (Gibco-BRL, Life Technologies, Paisley, U.K.) containing 10% fetal calf serum (FCS). PBMC were isolated by Ficoll-Hypaque centrifugation from blood samples, obtained from HIV-1 sero-negative and HIV-1-infected donors through the AIDS Center at Kaplan Medical Center. PBMC were stimulated with 5 μg/mL phytohemagglutinin (PHA) prior to use in infection experiments. HIV-1-infected PBMC were cultured for 3−4 days without PHA stimulation. HIV-1 clade B (T-tropic) primary clinical isolate, HIV-1 III_B and HIV-1 2D laboratory strains, as well as 3′-azido-3′-deoxythymidine (AZT), 2′,3′-dideoxy-3′-thiacytidine (3TC) (both are nucleoside HIV-1 RT inhibitors), and UC781 (non-nucleoside RT inhibitor) resistant HIV-1 clinical isolates were propagated by subculture in CD4+ MT2 cells. HIV-1 Ba-L and HIV-1 JF-RL were propagated in cMAGI cells. HIV-1 clade C primary clinical isolate was propagated by subculture in U937 cells. Aliquots of cell free culture supernatants were generally used as viral inocula.

NeoR was dissolved directly in the RPMI medium. Cytotoxicity determinations were carried out with the tetrazolium-based colorimetric assay (MTT assay), using a cell proliferation kit (CellTiter 96 Aq_{ueous} One solution cell proliferation assay, Promega). Viral growth was assessed by measurement of cell viability using the MTT assay, by assaying the RT activity levels in the culture supernatants (see below) and/or by measuring HIV-1 p24 antigen levels (p24 antigen capture kit, SAIC Frederick, Frederick, MD), according to the manufacturer's instructions. Cytopathic effects of HIV infection of CD4+ MT2 cells were also analyzed by microscopic assessment of syncytium formation. The latter data were obtained by analysis of duplicate samples by two independent observers.

Inhibition of HIV-1 Infection by NeoR. MT2 cells or PBMC were incubated at 37 °C with a multiplicity of infection of HIV-1 of 0.2−0.5 in the presence or absence of NeoR for several days without washing (protocol 1). Alternatively, after incubation for 2 h at 37 °C with the virus, cells were washed and cultured in the presence or absence of NeoR in the medium for several days (protocol 2). In a third protocol of infection (protocol 3), the cells were infected with HIV-1 in the presence or absence of NeoR for 2 h at 37 °C, washed, and then cultured for several days in the absence of NeoR. In all protocols, half of the medium was exchanged every 2 or 3 days with fresh medium, containing the appropriate concentration of NeoR. The concentrations that caused 50% inhibition of viral production (EC_{50}) were determined. In some experiments, the antiviral effect of

NeoR alone, AZT alone, or a combination of both antiviral compounds was examined.

Reverse Transcriptase Assay. Samples of culture medium from the infected cells were collected and clarified from cell debris by centrifugation at 5000*g* for 5 min. To 50 μL of clarified medium samples was added 50 μL of RT cocktail to the following final concentrations: 50 mM Tris-HCl (pH 8.0), 2.5 mM $MgCl_2$, 150 mM KCl, and 0.5 mM EGTA (BDH, Dorset, U.K.), 0.05% Triton X-100, 5 mM DTT (dithiothreitol, Sigma), 2% ethylene glycol, and 2.5 μg of an annealed poly-rA/oligo-dT (Sigma) template, and 5 μCi of ^{3}H-labeled TTP (specific activity of 50 Ci/mmol, Amersham-Pharmacia, Piscataway, NJ). The reaction mixture was incubated at 37 °C for 2 h or overnight. Following the incubation, 900 μL of 10% ice-cold trichloroacetic acid (TCA, Sigma) was added to the reaction mixture. Then the samples were incubated for 15 min on ice and transferred onto nitrocellulose filters (0.2 μm, Millipore, Bedford, MA), and the filters were washed several times with 10% ice-cold TCA on a manifold device (Sigma). The filters were dried and transferred to scintillation vials, and the amount of radioactivity was counted with a Kodak LC counter by using UltimaGold scintillation liquid.

Inhibition of Tat-Induced HIV-1 Production by the Infected Cells. Chronically infected H9 cells, or PBMC from HIV-1-infected individuals with high plasma viral loads, were washed twice with PBS by centrifugation at 400*g* for 10 min and seeded in 96-well plates (Nunc, Rosklide, Denmark) at a density of 75 000 cells per well in 200 μL of RPMI, with 10% FCS. The viral production from chronically infected cells was stimulated by addition of 10−20 nM recombinant HIV-1 Tat protein to the culture medium. The cells were incubated in the presence of varying concentrations of NeoR for 3 days at 37 °C. The inhibitory effect of NeoR on Tat-stimulated viral production was studied by measuring the RT activity in the supernatants after incubation for 2 or 3 days.

Inhibition of Tat-Dependent LTR-Driven Luciferase Activity. NeoR's ability to inhibit Tat−TAR interaction was determined in cell culture by an HIV-1 Tat-dependent bioluminescence bioassay based on adenoviral vectors (*32*). Briefly, crude HIV-1 Tat protein extract (25 μL) and adenoreporter virus (Ad-HIVluc, 10^{-3} dilution), containing a Tat-regulated luciferase reporter gene, were added simultaneously to cMAGI cells, cultured in 96-well plates in medium with or without NeoR. An adenovirus vector (Ad-HIVΔ-TARluc), in which the Tat responsive element (the TAR region) was deleted, was added instead of the Ad-HIVluc virus as a control for Tat-independent activation of the luciferase gene. After overnight incubation at 37 °C in a humidified 5% CO_2 incubator, luciferin (Boehringer Mannheim, Indianapolis, IN) dissolved in 60 mM Tris-acetate buffer (pH 7.5) was added to the culture medium to a final concentration of 0.3 mM. After incubation for 30 min at 37 °C, the cells were lysed with cell culture lysis reagent (CCLB, Promega), and the luciferase activity in the cells extracts was measured by adding 100 μL of luciferase assay reagent (Promega) and recording the emitted light with a Lucyl microplate luminometer (Anthos Labtec Instruments GmbH, Salzburg, Austria).

The crude Tat protein extract was prepared from 293/TAT cells, stably transfected with a Tat expression vector as described previously (*32*).

Interaction of Tat Protein and NeoR with CD4, CXCR4, and CCR5 Receptors. Measurement of the activity of the CD4 receptor and chemokine receptors CXCR4 and CCR5 on nonactivated or PHA-, interleukin-2 (IL-2)-, or Tat-activated PBMC was performed by flow cytometry (FACScan, Immunocytometry Systems, Becton Dickinson, San Jose, CA). Cells were activated by incubation with PHA or Tat for 24 h, or with IL-2 for 2−3 days at 37 °C in the presence or absence of NeoR. Following the activation, 0.5×10^6 cells were washed in ice-cold phosphate-buffered saline (PBS) containing 0.1% sodium azide (wash buffer) and incubated for 30 min at 4 °C with anti-CXCR4 monoclonal antibody (mAb), 12G5, conjugated to phycoerithrine (PE), anti-CCR5 mAb, 2D7 (PharMingen, San Diego, CA), B-F5 anti-CD4 mAb (Immuno Quality Products, Groningen, Netherlands), or Leu-3a (Becton Dickinson), conjugated to fluorescein isothiocyanate (FITC), in the absence or presence of stromal cell derived factor 1α (SDF-1α, R&D Systems, Minneapolis, MN), and different concentrations of NeoR. Nonspecific fluorescence was assessed by using isotype-matched controls. For double-staining experiments, the cells were incubated with PE-conjugated anti-CD14 mAb (PharMingen) and FITC-conjugated CXCR4 or CCR5 mAbs. Following the incubation with the antibodies, the cells were washed with ice-cold wash buffer and fixed in PBS containing 1% paraformaldehyde. For each sample, 10 000 events were acquired. Gated acquisition was assessed by a combination of gates based on either forward and side scatters or CD14-PE staining. Data were analyzed and processed using CellQuest software (Becton Dickinson).

Viral Binding Assay. To measure NeoR's ability to inhibit viral binding to cells, HIV-1 viral particles were radioactively labeled by endogenous reverse transcription (ERT), without detergent or amphipathic peptide-induced permeability of the viral envelope, in order not to perturb the virions, according to the method of Zhang et al. (*33*) and as previously described (*34*). Briefly, 0.5 mL of HIV-1 particles (1.5−5 ng of p24) was added to 0.5 mL of ERT reaction mixture [final concentrations of 10 mM Tris-HCl (pH 8.0), 150 mM NaCl, 1 mM $MgCl_2$, 50 μM dATP, 50 μM dTTP, 50 μM dCTP, and 50 μM dGTP, as well as 50 μCi of [α-^{32}P]dATP]. After incubation for 2 h at 37 °C, the reaction mixture was diluted with PBS to 2 mL, and the viral particles were concentrated to a final volume of 50 μL using a Centricon YM-50 centrifugal concentrator (Millipore), according to the manufacturer's directions. This procedure was repeated four times to remove unbound radiolabel. The viral particles were incubated for 2 h at 37 °C with 200 000 MT2 or U937 cells in 0.5 mL of RPMI with 10% FCS in the presence of various concentrations of NeoR. Following the incubation, the cells were washed twice with PBS by centrifugation at 400*g* for 10 min. The pellets were resuspended in PBS and transferred onto glass fiber filters (Millipore). The filters were washed twice with PBS, dried, and counted as described above.

PBMC Proliferation Assay. PBMC (100 000 cells per well) were seeded in a 96-well plate (Nunc) in 200 μL of RPMI with 10% FCS, containing 1 μL of anti-CD3 beads (PharMingen), as well as 0−20 nM Tat and 0−5 μM NeoR in each well. After incubation for 2 days at 37 °C, 1 μCi of [^{3}H]thymidine (Amersham) was added to each well and the cells were incubated for an additional 14 h. Then the cells were harvested on glass fiber filters (Millipore). The filters

were washed several times with water and were counted as described above.

CD8 Expression on PBMC. PBMC were activated by incubation with different concentrations of Tat for 24 h at 37 °C in the presence or absence of NeoR. The cells were stained with FITC-conjugated anti-CD8 mAb (PharMingen). Following the incubation with the antibodies, the cells were treated as described above and CD8 expression was analyzed by FACS. Nonspecific fluorescence was assessed by using an isotype-matched antibody control.

Modeling of the Complex between NeoR and TAR RNA. Several initial model structures of the complex of NeoR with TAR RNA were constructed, based on the experimental structure of TAR RNA in complex with arginine, as determined by NMR spectroscopy (PDB entry 1arj). Thus, each of the arginine side chains of NeoR was placed within the binding cavity of TAR RNA like the arginine in the experimental complex. Each of the structures was energy minimized using the Discover module of MSI (MSI Inc., San Diego, CA) and the CVFF force field. The positions of the TAR RNA atoms, except hydrogen, were fixed in these computations. In addition, we constrained the distances between the appropriate arginine NH_2 groups and the hydrogen bond acceptors, N7 and O6, of guanine 26. These hydrogen bonds correspond to the ones formed by the guanidino group of arginine in its complex with TAR RNA (1arj). The structure of one of the complexes, in which the arginine bound to ring I of NeoR interacts with guanine 26 of TAR RNA, was further optimized by several intermittent dynamics and minimization stages. Each dynamics stage included 5000 steps of 1 fs each. Each dynamics stage was followed by an energy minimization stage requiring that the maximum derivative be less than 0.001. In addition to the process described above, NeoR was placed in the minor groove of TAR RNA, like neomycin in the complex of TAR RNA with neomycin [PDB entry 1qd3 (*25*)]. This structure was energy minimized as well, with the positions of the TAR RNA atoms, except hydrogens, fixed.

RESULTS

Chemical Characterization of Neomycin B−Arginine Conjugate (NeoR). The major HPLC peak of ~90% purity, proven by mass spectroscopy (MALDITOF) to be *m*/*z* 1552.68, stands for the hexaarginine derivative of neomycin B (calculated mass of 1552.1). The ^{1}H NMR (400 MHz, D_2O) spectrum of NeoR (acetate salts) revealed the presence of the characteristic groups of the arginine moieties at chemical shifts (δ) of 3.59 (H_α) and 3.21 ppm (H_β) as well as at 1.64 and 1.82 ppm ($H_{\gamma,\delta}$). The characteristic neomycin B proton signals were observed, in particular, the anomeric hydrogen signals as doublets at 5.1, 5.3, and 5.73 ppm. Integration afforded a 1:6 ratio of antibiotic to arginine components. A ^{13}C NMR (100 609 MHz, 10% D_2O, proton-decoupled) spectrum of NeoR revealed carbon resonances of the C-arginine amide moieties at 20.68, 26.85, 36.91, and 50.2 ppm as well as carbon resonances of the neomycin moiety with the characteristic signals of the anomeric carbons at 92.005, 95.01 (pyranoside), and 105.61 ppm (furanoside). The spectrum also revealed a group of amide carbon resonances at 178.09 ppm and a guanidinium carbon signal at 154.56 ppm.

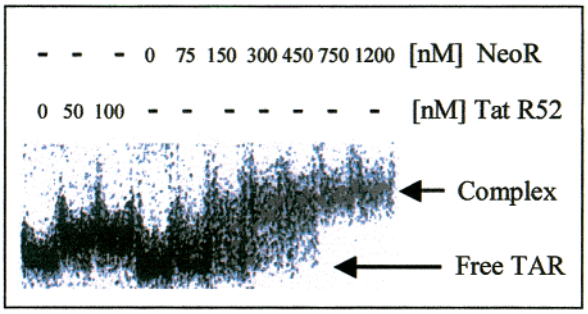

FIGURE 2: Electrophoretic mobility shifts of ^{32}P-labeled TAR RNA bound to NeoR in comparison to Tat-derived basic peptide R52. The TAR RNA concentration is 12 nM.

Binding of NeoR to HIV TAR RNA in Vitro. The ability of NeoR to bind TAR RNA was studied by using a gel shift technique as previously described (*21*, *28*, *29*). NeoR binding to ^{32}P-labeled TAR RNA was observed as electrophoretic band shifts (Figure 2). The conjugate displayed high affinity for TAR RNA (CD_{50} ~ 130 nM). The CD_{50} of the TAR RNA−Tat R52 peptide complex under the same conditions is ~50 nM (*28*). So far, NeoR exhibits the highest affinity for TAR RNA compared to the other AAC (*28*, *29*).

Fluorescence anisotropy is often used to measure dissociation constants of RNA−ligand interactions (*30*, *31*). It is well-known that not only Tat peptides bind TAR RNA with high affinity, but the Rev peptide does also (*35*, *36*). Using the fluorescence anisotropy technique and RevRh as the fluorescent probe, we found straightforward competition of NeoR and RevRh for TAR RNA binding with a K_D of 5.8 nM, indicating a high affinity of NeoR for TAR RNA comparable to that of RevRh (18.7 nM) and that of the natural ligand Tat_{49-57} (K_d = 6 nM). Thus, the possibility that NeoR could also bind to HIV-1 RRE RNA has been investigated using a fluorescence anisotropy assay. Preliminary results show that NeoR competes with RevRh for binding to RRE IIb with a K_D of 18.1 nM, similar to that of RevRh (K_d = 14.4 nM) (Figure 2 of the Supporting Information). These preliminary results are not surprising since NeoR mimics Tat and, as already mentioned (*33*, *36*), Tat also binds to HIV-1 RRE RNA.

Cellular Uptake of the Fluorescently Labeled Conjugate of NeoR. Uptake of fluorescently labeled AAC by live cells of different origins and their cellular distribution were described previously (*28*, *29*). Confocal microscopy of live PBMC and rat hippocanpal neurons, incubated for 30 min with the fluorescent derivative of NeoR (NeoR−FITC) at 0.5 μM, revealed that NeoR readily penetrates the cells and accumulates in the nuclei (Figure 3).

Anti-HIV Activity of NeoR. Addition of NeoR during the infection and thereafter (protocol 1; see Experimental Procedures) inhibited a variety of syncytia-inducing (T-tropic) laboratory and clinical HIV-1 isolates, including AZT, 3TC, and UC781 resistant HIV strains, with EC_{50} values of 1.7−5.3 μM (Table 1). Similarly, NeoR inhibited HIV-1 JR-FL and HIV-1 Ba-L (non-syncytia-inducing laboratory isolates) with EC_{50} values of 0.8 and 5 μM, when tested in U937 and cMAGI cells, respectively (Table 1). The inhibitory effects of NeoR on HIV-1 clade C infection in MT2 cell, under different incubation protocols, are presented in Figure 4. When the infection of the cells was performed in

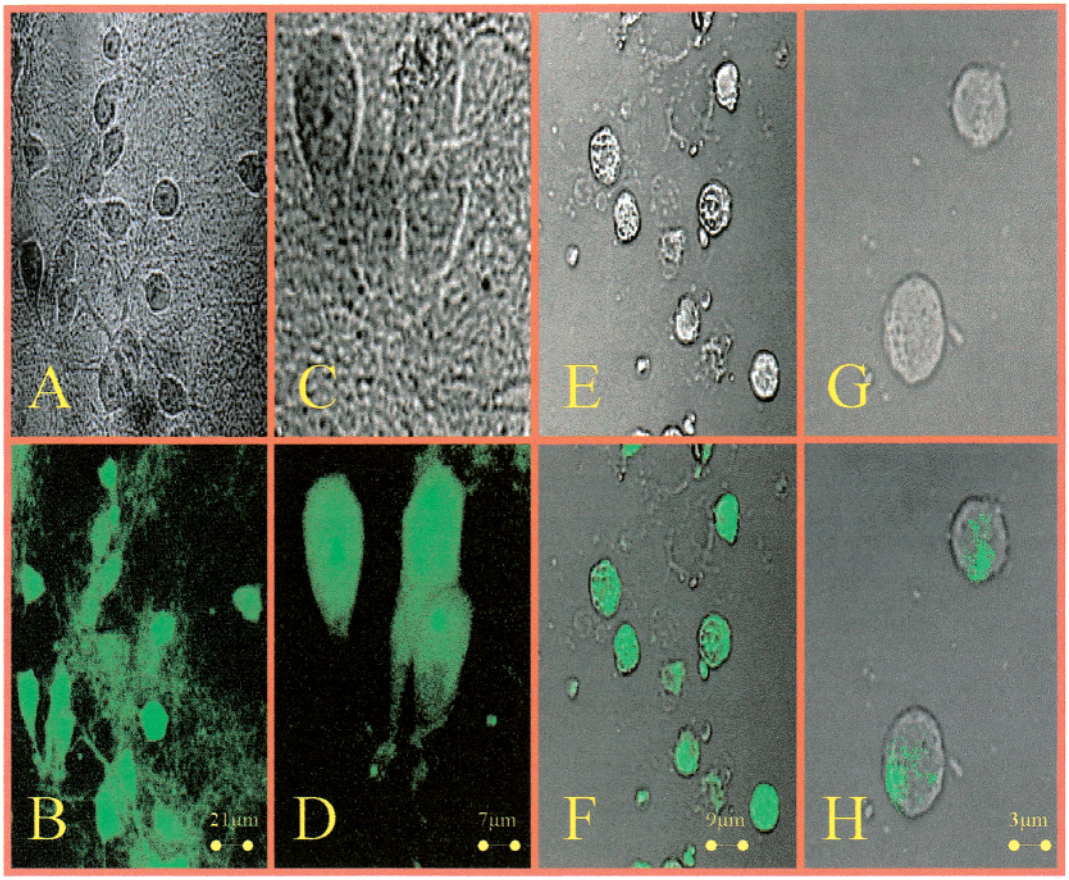

FIGURE 3: Confocal microscopy images of live rat hippocampal neurons and human PBMC stained with the NeoR−FITC conjugate. Images were taken with a 63× water immersion objective. The cells were incubated for 30 min with 0.5 μM NeoR−FITC conjugate. (A and C) Optical microscopy of the neurons. (B and D) Same fields as panels A and C, with confocal fluorescent microscopy at 488 nm excitation. Notice in panel D the localization of fluorescence in the nuclei. (E and G) Optical microscopy of PBMC. (F and H) Same fields as panels E and G, with confocal fluorescent microscopy at 488 nm excitation.

Table 1: Antiviral Activity of NeoR against HIV-1 Clinical Isolates and Laboratory Strains

		EC_{50} (μM)[a]												
		HIV-1 laboratory strains						HIV-1 clinical isolates						
		IIIB			2D	JR-FL	Ba-L	clade B			clade C		CC_{50}	
protocol[d]	cells	wt[e]	AZTr[f]	UC781r[g]	wt	wt	wt	wt[e]	AZTr[f]	AZT/3TC[h]	SI[i]	NSI[j]	(μM)[b]	TI_{50}[c]
1	MT2	3.7	2.7	1.7	2.3	–	–	2.3	5.3	3.6	1.8	–	275	94
3	MT2	3.2	3.3	2.9	4.1	–	–	4.2	5.2	8.4	2.9	–	–	–
1	PBMC	4.2	3.9	2.0	4.7	–	–	–	–	–	5.3	–	500	125
1	U937	–	–	–	–	0.8	–	–	–	–	–	0.9	–	–
1	cMAGI	–	–	–	–	–	5.0	–	–	–	–	–	–	–

[a] The 50% effective concentration which inhibited HIV-1 replication was determined by reverse transcriptase or p24 antigen levels. The data are the average of two independent experiments carried out in duplicate. [b] The 50% cytotoxic concentration in MT2 and PBMC was determined by a tetrazolium-based colorimetric assay. [c] The 50% in vitro therapeutic index was calculated by dividing the CC_{50} by the average EC_{50}. [d] In protocol 1, NeoR was present throughout the experiment. In protocol 3, NeoR was present during the first 2 h, and then washed. [e] Wild-type virus. [f] HIV-1 isolate resistant to AZT. [g] HIV-1 isolate resistant to UC781, a potent non-nucleoside RT inhibitor. [h] HIV-1 isolate resistant to AZT and 3TC. [i] HIV-1 isolate which induced syncytium formation. [j] HIV-1 clincal isolate which does not induce syncytium formation.

the absence of NeoR (protocol 2), the EC_{50} values were somewhat higher (Figure 4) than in protocol 1. However, the presence of NeoR only during the first 2 h of infection (protocol 3) was sufficient for inhibition of the viral proliferation.

The antiviral activity of NeoR against laboratory strain HIV-1 2D and clade C clinical isolate in the presence of AZT was found to be additive to that of AZT (data not shown). The 50% cytotoxic concentrations (CC_{50}) of NeoR were 275 μM in MT2 cells and 500 μM in PBMC (Table 1). Thus, the 50% therapeutic index (TI_{50}, which is the CC_{50}/EC_{50} ratio) of NeoR is 94 and 125 in MT2 cells and PBMC, respectively (Table 1).

Effect of NeoR on Viral Binding to Cells. The finding that the presence of the NeoR only during the first 2 h of infection was enough to inhibit virus production (Figure 4) suggests that NeoR may interfere with the binding of the virus to the cells. To test if NeoR also inhibits HIV-1 binding to cells, we used ^{32}P-labeled (see Experimental Procedures) HIV-1 III_B virions and incubated them for 2 h with MT2 cells in the presence or absence of different concentrations of NeoR up to 16 μM (figure not shown). NeoR efficiently inhibited,

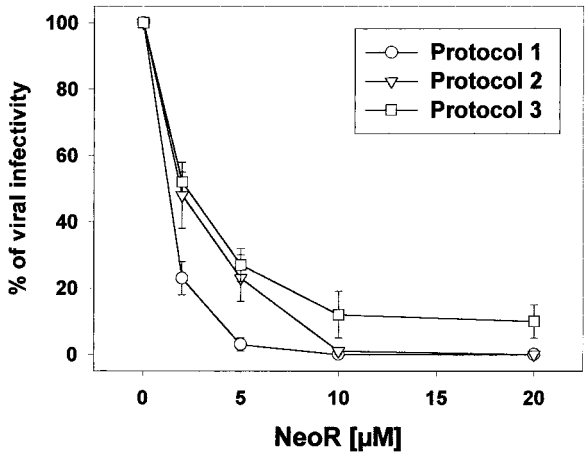

FIGURE 4: Inhibitory effect of NeoR on the replication of HIV-1 clade C infection in MT2 cells. MT2 cells were infected for 2 h at 37 °C in the absence or presence of 2−20 μM NeoR followed by cell wash. Approximately 5 × 10^4 infected cells were seeded per well in a 96-well plate and were incubated for 4 days in the absence or presence of 2−20 μM NeoR, until syncytia were observed (>25% cpe). Cell viability was measured by the tetrazolium-based colorimetric method. The results that are shown are means ± standard deviation of triplicate experiments. (○) NeoR was present during the infection step and after the cells were washed. (▽) NeoR was present only after the cell wash. (□) NeoR was present only during the first 2 h, before the cells were washed.

in a dose-dependent manner, the binding of the labeled virions to the cells; e.g., the level of viral binding to cells was reduced by 75% in the presence of 4 μM NeoR, and almost abolished in the presence of 8 μM NeoR.

Interaction of NeoR with CD4, CXCR4, and CCR5 Receptors. CD4 is the main receptor of HIV-1, while CCR5 and CXCR4 are the main coreceptors for entry of HIV-1 M-tropic and T-tropic viruses into the cells, respectively (reviewed in refs *37* and *38*). Since NeoR inhibited HIV-1 binding to cells, we examined whether NeoR can interact with these receptors, by testing its capacity to inhibit the binding of monoclonal antibodies against them. While NeoR did not inhibit the binding of B-F5 or Leu-3a mAb against CD4 or the 2D7 mAb to CCR5, 2.5 and 5 μM NeoR caused 66 and 91% inhibition of 12G5 mAb binding to CXCR4 in PBMC, respectively, as determined by the median fluorescence intensities (Figure 5a). While similar competition with 12G5 mAb binding to CXCR4 was seen with SDF-1α, the natural ligand of CXCR4, no inhibition at all of 12G5 mAb binding to CXCR4 was found in the presence of 10 μM neomycin (data not shown).

Effect of NeoR on Extracellular Tat Activities. (1) Competition of NeoR with HIV-1 Tat for Binding to CXCR4. HIV-1 Tat also binds to CXCR4 (*9*). As shown in Figure 5b, Tat inhibited binding of the NeoR−FITC conjugate to PBMC, probably by competing with NeoR for binding to CXCR4. Similar results were obtained whether the cells were first incubated for 24 h with PHA or used immediately after fractionation from whole blood (data not shown).

(2) Inhibition of Tat Transactivation. It is known that soluble Tat protein is taken up by cells and is transported to the nuclei, where it transactivates the transcription from the HIV-1 long terminal repeat promoter (*39*). To test the capacity of NeoR to inhibit Tat enhancement of HIV-1 production in cell culture, we used H9 cells chronically infected with HIV-1. As shown in Figure 6, NeoR, in the

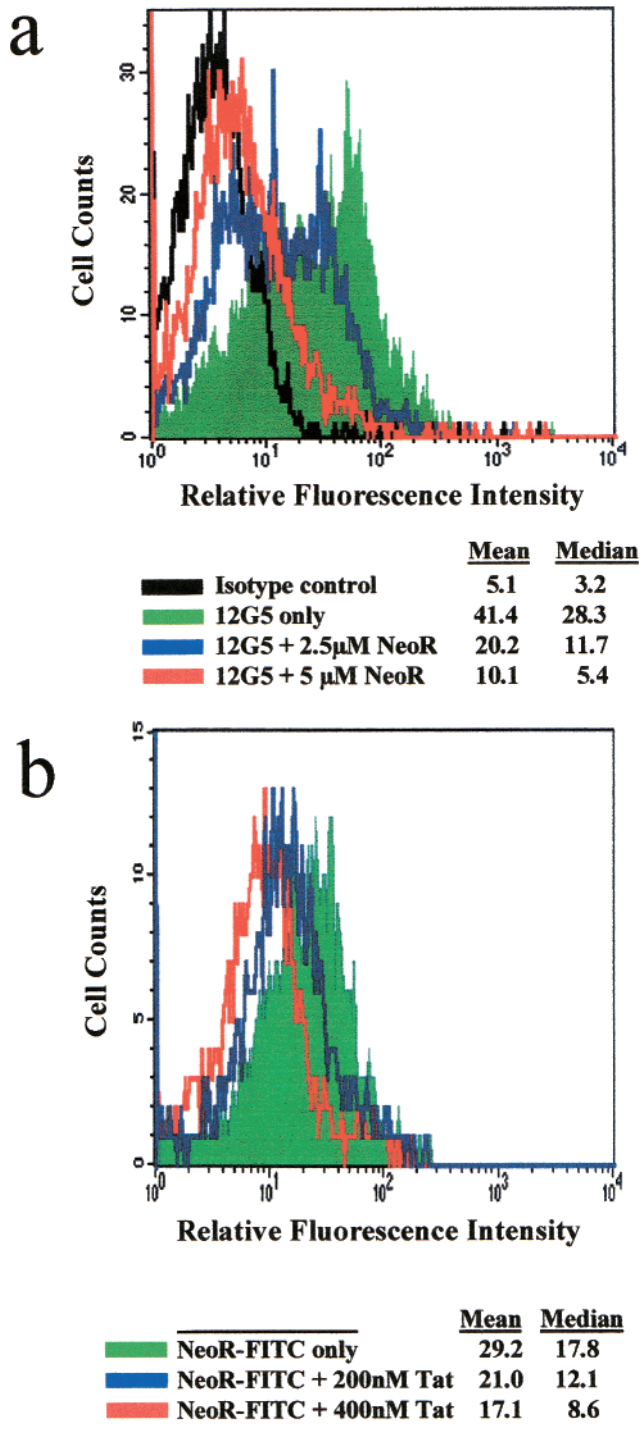

FIGURE 5: (a) Competition of NeoR and 12G5 mAb binding to CXCR4 on PBMC. Cells were incubated with PE-conjugated isotype control mAb, PE-anti CXCR4-conjugated mAb (12G5) alone or in the presence of 2.5 or 5 μM NeoR for 30 min at 4 °C. The cells were then washed twice with PBS and analyzed by flow cytometry. The mean and median fluorescence intensities are shown in the legend. (b) Inhibition of entry of the NeoR−FITC conjugate into PBMC by HIV-1 Tat. PBMC were incubated with ∼0.5 μM NeoR−FITC in the presence of 0, 200, or 400 nM HIV-1 Tat for 30 min at 4 °C. The cells were then washed twice with PBS and analyzed by flow cytometry. The mean and median fluorescence intensities are shown in the legend.

absence of added extracellular Tat, inhibited viral production, with an EC_{50} value of ∼2.5 μM, suggesting that NeoR inhibits the intracellular Tat produced in the HIV-1-infected cells. Addition of extracellular Tat significantly stimulated

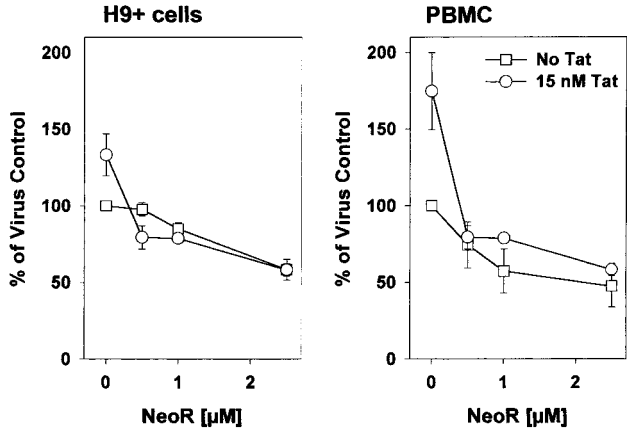

FIGURE 6: Inhibitory effect of NeoR on Tat-induced transactivation of viral production by H9 cells chronically infected with HIV-1 and PBMC from an HIV-1-infected individual with a high viral load. The cells were incubated in the absence (□) or presence (○) of 15 nM Tat and 0−2.5 μM NeoR. The level of viral production was measured by reverse transcriptase activity in supernatants during the third day of incubation. The results represent one of two similar experiments, and the data that are shown are the means ± standard deviation of triplicate samples.

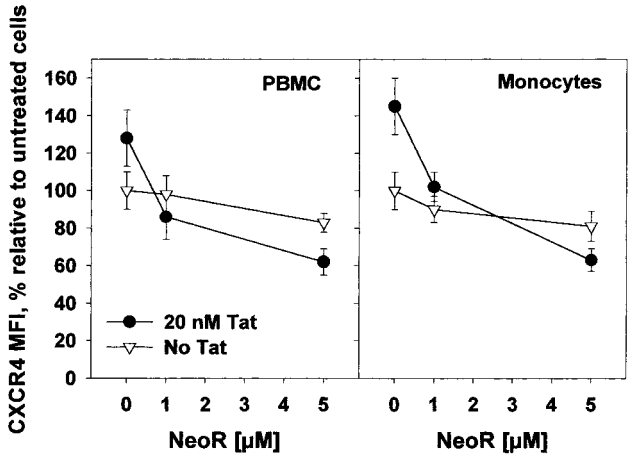

FIGURE 7: Inhibitory effect of NeoR on Tat-induced CXCR4 expression upregulation on PBMC and monocytes. PBMC were plated and treated with 20 nM Tat (●) or Tat diluent buffer (untreated) (▽) in the presence of 0−5 μM NeoR. After incubation for 24 h, the cells were collected, washed to remove the extracellular drugs, and analyzed for CXCR4 expression by flow cytometry. The data represent averages of four independent experiments; the level of surface CXCR4 expression is calculated as median fluorescence intensity values, taken relative to the untreated control.

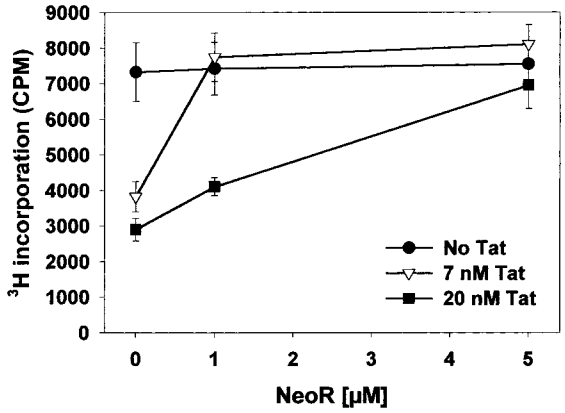

FIGURE 8: Effect of NeoR on Tat-induced suppression of the proliferative response of PBMC to CD3 activation. PBMC from an HIV-negative donor were activated by incubation with anti-CD3 beads and incubated with 0 (●), 7 (▽), or 20 (■) nM Tat for 24 h in the presence of 0, 1, or 5 μM NeoR. The proliferative response was measured by the level of [^{3}H]thymidine incorporation into the cells. The results shown are means ± standard deviation of triplicate experiments.

HIV-1 production by the cells. However, 0.5 μM NeoR abolished this enhanced production of HIV-1 induced by Tat (Figure 6). Similar results were obtained with PBMC from an HIV-1-infected individual with a high plasma viral load (more than 580 000 HIV RNA copies/mL) (Figure 6), suggesting that NeoR targets the Tat transactivation step in the HIV life cycle and the extracellular Tat upregulation of HIV-1 viral entry coreceptor expression. To corroborate this possibility, the direct inhibition of Tat−TAR interaction by NeoR was examined by using a highly sensitive adenoviral HIV LTR-mediated luciferase gene expression bioassay. The assay system consists of two adenoreporter vectors, one of which is responsive to HIV-1 Tat protein activity (Ad-HIVluc), and the second of which is not (Ad-HIV Δ-TAR-luc), by virtue of a deletion of the TAR site within the HIV LTR. In the absence of NeoR, addition of 25 μL of crude Tat protein extract to cMAGI cells transfected with an HIV LTR-driven luciferase reporter gene increased the amount of emitted light from 1670 to 28 159 light units. In the presence of NeoR (0−20 μM), the amount of emitted light was reduced up to 80% with an IC_{50} of 10 μM. In contrast, the light emitted by cMAGI cells transfected with Ad-HIVΔ-TARluc was not affected by the addition of Tat and/or 20 μM NeoR (20 μM NeoR was not toxic to the cells).

(3) Inhibition of Tat Upregulation of CXCR4 Coreceptor Expression on Lymphocytes and Monocytes. Incubation of T-cells in the presence of Tat protein was shown to upregulate the expression of chemokine coreceptors of HIV viral entry (*12*), as soon as 4−24 h after Tat addition to the cell culture medium (*13*, *14*), and is sustained for 8 days (*12*). We examined the effect of NeoR on the expression of CXCR4 on different PBMC subsets following treatment of the cells for 24 h with 20 nM Tat. Only a minor effect on the proportion of the cells expressing CXCR4 was noted when PBMC were cultured in the presence of 20 nM Tat or Tat diluent buffer for 24 h. However, the median fluorescence intensity, which reflects the number of membrane receptors expressed per cell, was increased by 20 and 45% on the Tat-treated lymphocytes and monocytes/macrophages, respectively (Figure 7). This upregulation by Tat was abolished by 1 μM NeoR (Figure 7).

(4) Inhibition of PBMC Proliferation Suppression by Tat. Tat protein suppresses lymphocyte proliferation (*2*). To study the capacity of NeoR to inhibit this immunosuppressive effect of Tat, we activated PBMC of HIV sero-negative donors with anti-CD3 Ab and incubated the cells with 7 or 20 nM Tat. The addition of Tat resulted in a significant reduction in the extent of PBMC proliferation (∼50−60%), as determined by ^{3}H thymidine incorporation (Figure 8). As shown, 1 and 5 μM NeoR abolished the antiproliferative effect of 7 and 20 nM Tat, respectively (Figure 8).

(5) Inhibition of Induction of CD8 Expression by Tat. One of the possible mechanisms of Tat-induced immunosuppression is induction of CD8+ suppressor T-cells (*40*). To investigate the ability of NeoR to inhibit this effect of Tat, we incubated nonactivated PBMC, obtained from six

HIV sero-negative donors, with 15 nM Tat for 24 h at 37 °C in the presence or absence of various concentrations of NeoR. HIV-1 Tat caused in all six experiments an increase in the range of 23−69% in the level of CD8 expression, as determined by the median fluorescence intensities, in comparison to untreated controls. In all these experiments, 1 μM NeoR inhibited significantly the Tat-induced upregulation of CD8 expression (78 ± 20.7% inhibition of the increase in the median fluorescence intensities). A representative experiment is available upon request in the form of Supporting Information (Figure 3).

DISCUSSION

Development of inhibitors against the HIV transcriptional transactivator protein, Tat, is highly important and might even be critical in the fight against AIDS. Indeed, several Tat-mimetic peptide/peptoid compounds that target TAR RNA and demonstrate a pronounced antiviral activity have recently been described, such as a D-amino acid peptide derived from the Tat basic domain (*41*), CGP64222 (*42*), and AAC (*29*). It was also reported (*29*) that AAC bind to TAR RNA with high affinity, but not to a variety of short RNA oligonucleotides and truncated TAR RNA sequences (in the micromolar concentration range). An ∼10-fold excess of yeast RNA inhibits formation of the AAC−TAR complex, similar to the effect of tRNA on Tat-derived peptide binding to TAR. Here we present a novel HIV-1 Tat mimetic, a hexaarginine derivative of neomycin B (NeoR) (*43*), that not only binds TAR and inhibits the binding of HIV-1 to cells but also manifests potent inhibition of several detrimental extracellular Tat activities. The selection of neomycin B for the synthesis of NeoR was based on the ability of neomycin B to bind TAR RNA, although with a very low affinity (*24*), in contrast to the nonactive aminoglycoside antibiotics kanamycin A and gentamicin C. The synthesis, anti-HIV activities, and, in particular, the inhibition of the extracellular activities of Tat by NeoR are presented.

Competition of NeoR with Tat Functions. Since NeoR is a Tat mimetic, we examined its ability to compete with several Tat functions, especially those dependent on the Tat basic domain. As we demonstrate here, NeoR (0.5 μM) caused a 50% reduction in the level of enhanced production of HIV-1 induced by Tat in H9 T-cells chronically infected with HIV-1 and of PBMC infected with HIV-1, indicating that NeoR interferes with Tat transactivation activity. NeoR inhibition of Tat−TAR interaction-driven luciferase-reported gene activity supports the notion that NeoR also interacts in vivo with TAR. Unpublished preliminary results showing that resistance by HIV-1 to NeoR involves mutations in the TAR region further strengthen this notion. The fact that significantly higher concentrations of NeoR are needed in vivo than in in vitro to inhibit Tat−TAR interactions is not surprising, since NeoR may interact with other molecules, such as a Tat cofactor, lowering the number of "available" NeoR molecules that may compete with Tat for TAR binding. The capacity of Tat to upregulate CXCR4 expression on lymphocytes and monocytes/macrophages (*12*−*14*) was abolished by 1 μM NeoR. A similar capacity to inhibit CXCR4 upregulation induced by Tat was recently reported for a stilbene derivative (*44*), a compound that directly binds Tat, but does not bind TAR RNA. Another Tat activity, the antiproliferative effect on CD3-activated PBMC (*45*), was also abolished by 1−5 μM NeoR, as presented in this report. Tat has also been found to induce CD8+ suppressor lymphocytes in vitro (*46*). The upregulation of CD8 expression on PBMC by Tat, presented in this report, may be the manifestation of this mechanism. Importantly, NeoR (1 μM) neutralized this activity of Tat as well, like what has been reported for anti-Tat antibodies (*46*). These results suggest competitive mechanisms of NeoR with Tat-induced immunosuppression.

Recently, it has been shown that extracellular HIV-1 Tat acts as a CXCR4 antagonist by binding to CXCR4 and at concentrations of 0.5−1 μM inhibits CXCR4-dependent HIV-1 infection (*9*, *47*). This, together with our findings that NeoR inhibits binding of mAb against CXCR4 (Figure 5a) and that the extracellular HIV-1 Tat inhibits NeoR−FITC uptake by PBMC (Figure 5b), suggests that both compete for the same target, the HIV-1 coreceptor CXCR4. However, the possibility of indirect interaction mediated by another factor(s) cannot be excluded.

NeoR Inhibits HIV-1 Binding to Cells. The presence of NeoR only during the first 2 h of cell exposure to HIV was sufficient to inhibit viral production. This raised the possibility that NeoR inhibits viral binding to cells and/or that sufficient amounts of NeoR are readily taken into the cells, which inhibit subsequent post-cell entry steps of the virus life cycle. As shown here, both possibilities occur: NeoR inhibits penetration into cells of radioactively labeled HIV particles, and NeoR, which is taken readily into cell nuclei, abolishes the enhancement of viral production in cells chronically infected with HIV-1, induced by Tat.

The mechanism of inhibition of T-tropic HIV-1 binding to cells by NeoR could also be via blockade of the CXCR4 coreceptor. The inhibitory effect of NeoR on binding of mAb 12G5 to CXCR4 supports this notion. A similar blockade of the CXCR4 coreceptor were found for the triarginine−gentamicin conjugate (R3G) and the tetraarginine−kanamycin conjugate (R4K), but not for the tetra-γ-guanidinobutyric acid−kanamycin conjugate (GB4K) (*48*). These results are in agreement with the finding that the Tat-peptoid CGP64222 inhibits the HIV replicative cycle also through a selective interaction with the HIV-1 coreceptor CXCR4 (*42*). The interaction between HIV-1 glycoprotein 120 (gp120) and the CXCR4 coreceptor involves a highly conserved arginine residue in hypervariable region 3 (V3 loop) of gp120 (*49*). T-tropic HIV-1-derived V3 loop peptides directly bind to CXCR4 and inhibit T-tropic HIV-1 interaction (*50*). Moreover, the Tat protein itself binds CXCR4 and even can block at high concentrations entry of HIV into the cells (*2*, *47*). Since NeoR is a Tat mimetic, comprising several arginine moieties, it may also compete with the gp120 V3 loop for CXCR4 receptor binding and thus inhibit entry of HIV-1 into cells. Although not shown here, recent results supporting this possibility show that 7 μM NeoR inhibits >90% gp120-mediated cell death. Structural mimicking of the gp120 V3 loop by NeoR, where three arginine moieties of NeoR are superimposed on arginines 8, 11, and 15 of the V3 loop of gp120 (*51*, *52*), can be easily achieved due to the flexibility of NeoR (not shown).

NeoR, like R3G, R4K, and GB4K (*48*), AMD3100 (*53*), and CGP64222 (*42*), does not inhibit the binding of 2D7 mAb against CCR5. However, NeoR and R3G inhibit HIV-1

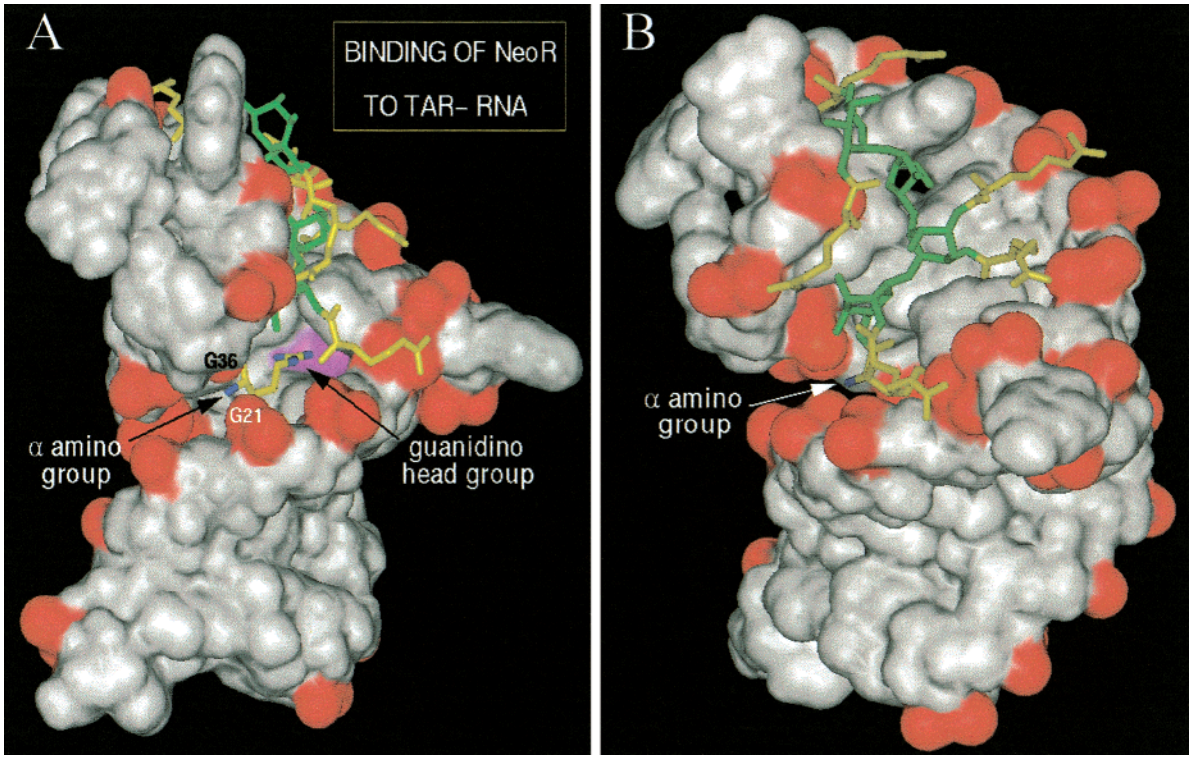

FIGURE 9: Plausible structure of the TAR−RNA complex with NeoR. Specifically, the arginine on ring I conjugated via the aliphatic amine of neomycin B is positioned in the cavity formed by the bulge of TAR RNA. The surface of TAR RNA is colored white, except for the phosphate groups, which are red. The neomycin core of NeoR is shown in green, and the arginine moieties are in yellow. The guanidino group of the arginine on ring I interacts with the N7 and O6 atoms of guanine 26, whose surface is shown in magenta. The α-amino group interacts with the O2P atoms of guanines 21 and 36 of TAR RNA. The structure of TAR RNA is based on the structure of the TAR RNA−arginine complex (PDB entry 1arj). Panel B is view after a ~90° clockwise turn of panel A.

Ba-L (a M-tropic viral isolate) with an EC_{50} values of 5 (Table 1) and 29 μM, respectively (*48*), while R4K, GB4K, and AMD3100 do not (*48*). Since Tat also upregulates CCR5 expression (*14*), NeoR, being a Tat mimetic, may abolish this effect in a manner similar to that shown for CXCR4. Thus, inhibition of the HIV-1 Ba-L replicative cycle by NeoR may be either by competitive reaction with extracellular Tat or through postentry events, such as inhibition of HIV Tat transactivation. Another possibility of viral binding inhibition is through interaction of NeoR with the CD4 receptor. However, NeoR does not inhibit the binding of B-F5 or Leu-3a mAb against CD4 in whole blood or in PBMC, as was also found for R3G (data not shown and ref *48*).

Molecular Modeling of the NeoR−TAR Complex. NeoR was designed as an HIV-1 Tat mimetic. This, together with (a) the interaction of NeoR with HIV-1 TAR RNA (shown by the gel shift assay), (b) a K_D of 5.8 nM (determined by fluorescence anisotropy), (c) the ability of NeoR to inhibit enhancement of HIV-1 production induced by Tat, (d) inhibition of Tat−TAR interaction (dependent biolumines-cence activity assay), and (e) preliminary results showing that resistance by HIV-1 to NeoR involves mutations in the TAR region, led us to study the possible modes of interaction between the two molecules.

A model structure of the TAR−neomycin complex based on NMR spectroscopy was recently calculated (*25*). The model suggests that neomycin binds in a pocket formed by the minor grove of the lower stem and the uridine-rich bulge of TAR, which adopt a conformation different from that known for Tat−TAR interactions (*26*, *27*). Thus, it was of interest to test whether the conformation of TAR adapted in the TAR−neomycin complex is adequate for binding the neomycin−arginine conjugate. To this end, we constructed a model structure with NeoR placed in the same binding pocket as neomycin. Energy minimization, however, pro-duced an unlikely complex, in which most of the contacts of the NeoR rings with the minor groove were lost. These results suggest that either the NeoR molecule does not bind in the minor groove of TAR RNA or a major conformation change in the RNA molecule is necessary for accommodation of the modified ligand.

An alternative mode of binding of NeoR to TAR RNA is through the arginine ends, imitating the TAR−RNA complex with arginine, where the ligand binds in a cavity formed by the bulge of the RNA (*26*, *27*). Each of the six arginine groups was placed in the arginine-binding cavity, and the six resulting complexes were energy minimized as described in Experimental Procedures. These computations converged smoothly and produced plausible structures, all characterized by the binding of one arginine group in the TAR RNA cavity and by numerous interactions of the rest of the NeoR molecule with the loop fragment of the RNA.

One of the resultant structures is shown in Figure 9. In addition to the hydrogen bonds between the guanidino moiety of the arginine side chain and the hydrogen bond acceptors, O6 and N7, in guanine 26, for which the distance constraints applied in the minimization called, one notes a strong electrostatic interaction between the α-amino group (the free amine group) of the same arginine with the phosphate groups of guanine 21 and guanine 36. The rest of the NeoR molecule

spreads over the shallow "bowl" formed by the loop segment of the RNA such that the neomycin rings interact with the RNA bases, while the arginine groups, except the one placed in the arginine-binding cavity, interact with the phosphate moieties. The latter interactions are probably nonspecific because in an aqueous solution the phosphate groups as well as the guanidino groups are likely to be hydrated. Interestingly, the interactions of the α-amino group with two phosphate groups and the general position of the neomycin rings on the surface of the TAR RNA molecule are similar in all six complexes formed when one of the arginine side chains is placed in the TAR RNA arginine-binding cavity. The accuracy of our computations is limited; hence, we cannot determine whether the binding in one complex is stronger than that in another one. Nevertheless, the modeling study provided a few important results, which were not foreseen and which are supported by the experimental results.

(a) The possibility of binding NeoR in the minor groove of TAR RNA, analogous to the binding of neomycin B (*25*), was discarded.

(b) NeoR binds to TAR RNA in a manner analogous to the binding of the arginine moiety of the Tat peptide to TAR RNA. This result complies with the experimental results. So far, arginine residues of aminoglycoside were properly recognized by TAR RNA (*28*, *29*). The linker between the "core" (e.g., neomycin B) and the "headgroup" (guanidino group) is most important for RNA binding.

(c) The strong interaction between the α-amino of the arginine moiety of NeoR and the TAR RNA phosphate group is a modeling prediction, which is experimentally supported (*28*, *29*). Thus, the affinity of GB4K, lacking an α-amino acid group in the linker, for TAR RNA was very low compared to that of the tetraarginine derivative, R4K (*28*, *29*). Also, GB4K anti-HIV activity in cell culture (*48*) and in equine infectious anemia virus (EIAV) in equine dermal fibroblasts (ED) was very low (*29*). Thus, all the above may explain the very low anti-HIV-1 activities and affinity of GB4K and other guandino derivatives for HIV-1 TAR RNA reported in ref *28* and of other guanidino derivatives of aminoglycosides for HIV-1 RRE RNA (*54*, *55*).

(d) The binding of NeoR to TAR RNA is predicted by the modeling study to be a combination of specific binding of one arginine moiety with the bulge of TAR RNA in addition to nonspecific interactions between the rest of NeoR and the loop segment of TAR RNA. This modeling prediction is supported by our recent studies (*29*). Our footprinting analysis suggested that GB4K-induced conformational changes in the loop region make this site more accessible for RNAse A cleavage. Nevertheless, GB4K cannot protect the major site, the bulge, or its conjunction to the upper and lower stem from RNAse A cleavage in contrast to Tat peptide R52 and AAC (*29*).

(e) Moreover, the model structure suggests that, at a given time, only one of the six arginine group of NeoR is bound to the major groove. The finding that the monoarginine derivative of neamine binds efficiently to TAR RNA with an IC_{50} of 600 nM (*56*) also supports our modeling study.

Interestingly, in a theoretical study of the Tat_{46-58}−TAR complex, Seewald et al. (*57*) present an interaction between Arg52 and the bulge of TAR and between Arg53 and two adjacent phosphates, P21 and P22. Hence, both our model and the Tat_{46-58}−TAR model identify two specific contacts in the vicinity of the bulge. However, in our model, both contacts originate from the same arginine (via the guanidino group and the α-amino group), whereas in the Tat_{46-58}−TAR model, two adjacent arginines are involved. This similarity can explain the anti-HIV and Tat antagonist activities of NeoR.

Conclusion. The rapid emergence of resistant HIV mutations represents a formidable challenge to the development of anti-HIV drugs. One way of overcoming or diminishing this severe problem is the development of a compound that can interact with several viral targets, and which may be an effective inhibitor of several stages of viral replication, since resistance to multitarget inhibitors would necessitate multiple mutations.

HIV-1 Tat protein plays one of the central roles in AIDS pathogenesis, due to its principle function in HIV-1 transcription and multiple involvement in HIV progression and immunosuppression. Therefore, the discovery of novel HIV Tat antagonists is not just one more strategy in anti-HIV pharmacological intervention, but may be highly important in view of the inability of existing therapies to eradicate HIV infection. Here we show for the first time the novel HIV-1 Tat mimetic antagonist NeoR, which in addition to inhibiting Tat transactivation and other HIV Tat extracellular detrimental functions, inhibits HIV binding to cells. Our data suggest that NeoR interferes with Tat transactivation by interacting with TAR RNA, and a plausible structure of the complex of TAR RNA with NeoR is described. In addition, we demonstrate the capacity of NeoR to inhibit several extracellular Tat activities, partially by competing with Tat for the binding to CXCR4. Finally, we demonstrate the capacity of NeoR to inhibit HIV-1 infection by interfering with HIV binding to cells, partially by binding with one of the main HIV-1 cellular coreceptors, CXCR4. Although it is not shown here, it is worth mentioning that NeoR is not toxic to mice given intravenously two single doses of 25 mg/kg of body weight over the course of 2 h (unpublished data).

We believe that NeoR, by its multitarget HIV-1 inhibitor nature, may be an attractive lead for the development of compounds that may help circumvent or reduce this immense obstacle in HIV-1 therapy.

ACKNOWLEDGMENT

We thank Prof. Zvi Bentwich (AIDS Center, Hebrew University, Rehovot, Israel) for his continued assistance and interest, Prof. Alik Honigman (Department of Virology, Hebrew University) for help with the HIV LTR-mediated luciferase gene expression bioassay, and Dr. E. Korkonan (Brain Research, Weizmann Institute of Science) for help with the confocal microscopy studies. The following reagents were obtained through the AIDS Research and Reference Reagent Program, Division of AIDS, NIAID, NIH: HIV Ba-L from Dr. Suzanne Gartner, Dr. Mikulas Popovic, and Dr. Robert Gallo; HIV-1 JF-RL from Dr. Irvin Chen; AZT and 3TC from Dr. Raymond F. Schinazi; and HIV-1 Tat from Dr. John Brady. The cMAGI cells were a generous gift from Dr. Phalguni Gupta (University of Pittsburgh, Pittsburgh, PA), and the HIV-1 clade B clinical isolates were a generous gift from Dr. Mark A. Wainberg (McGill AIDS Centre, McGill University, Montreal, PQ).

SUPPORTING INFORMATION AVAILABLE

Four figures depicting the HPLC trace of NeoR (Figure 1), anisotropy studies (Figure 2), the inhibition of Tat-dependent LTR-driven luciferase activity by NeoR (Figure 3), and the effect of NeoR on Tat-induced CD8 expression on PBMC (Figure 4). This material is available free of charge via the Internet at http://pubs.acs.org.

REFERENCES

1. Li, C. J., Ueda, Y., Shi, B., Borodyansky, L., Huang, L., Li, Y. Z., and Pardee, A. B. (1997) *Proc. Natl. Acad. Sci. U.S.A. 94*, 8116−8120.
2. Gallo, R. C. (1999) *Proc. Natl. Acad. Sci. U.S.A. 96*, 8324−8326.
3. Watson, K., and Edwards, R. J. (1999) *Biochem. Pharmacol. 58*, 1521−1528.
4. Noonan, D., and Albini, A. (2000) *Adv. Pharmacol. 48*, 229−250.
5. Cullen, B. R. (1998) *Cell 93*, 685−692.
6. Karn, J. (1999) *J. Mol. Biol. 293*, 235−254.
7. Ensoli, B., Buonaguro, L., Barillari, G., Fiorelli, V., Gendelman, R., Morgan, R. A., Wingfield, P., and Gallo, R. C. (1993) *J. Virol. 67*, 277−287.
8. Albini, A., Ferrini, S., Benelli, R., Sforzini, S., Giunciuglio, D., Aluigi, M. G., Proudfoot, A. E., Alouani, S., Wells, T. N., Mariani, G., Rabin, R. L., Farber, J. M., and Noonan, D. M. (1998) *Proc. Natl. Acad. Sci. U.S.A. 95*, 13153−13158.
9. Xiao, H., Neuveut, C., Tiffany, H. L., Benkirane, M., Rich, E. A., Murphy, P. M., and Jeang, K. T. (2000) *Proc. Natl. Acad. Sci. U.S.A. 97*, 11466−11471.
10. Zauli, G., Gibellini, D., Celeghini, C., Mischiati, C., Bassini, A., La Placa, M., and Capitani, S. (1996) *J. Immunol. 157*, 2216−2224.
11. Ross, T. M. (2001) *Leukemia 15*, 332−341.
12. Huang, L., Bosch, I., Hofmann, W., Sodroski, J., and Pardee, A. B. (1998) *J. Virol. 72*, 8952−8960.
13. Secchiero, P., Zella, D., Capitani, S., Gallo, R. C., and Zauli, G. (1999) *J. Immunol. 162*, 2427−2431.
14. Weiss, J. M., Nath, A., Major, E. O., and Berman, J. W. (1999) *J. Immunol. 163*, 2953−2959.
15. Boykins, R. A., Mahieux, R., Shankavaram, U. T., Gho, Y. S., Lee, S. F., Hewlett, I. K., Wahl, L. M., Kleinman, H. K., Brady, J. N., Yamada, K. M., and Dhawan, S. (1999) *J. Immunol. 163*, 15−20.
16. Goldstein, G. (1996) *Nat. Med. 2*, 960−964.
17. Gregoire, C. J., and Loret, E. P. (1996) *J. Biol. Chem. 271*, 22641−22646.
18. Truant, R., and Cullen, B. R. (1999) *Mol. Cell. Biol. 19*, 1210−1217.
19. Hauber, J., Malim, M. H., and Cullen, B. R. (1989) *J. Virol. 63*, 1181−1187.
20. Puglisi, J. D., Tan, R., Calnan, B. J., Frankel, A. D., and Williamson, J. R. (1992) *Science 257*, 76−80.
21. Calnan, B. J., Tidor, B., Biancalana, S., Hudson, D., and Frankel, A. D. (1991) *Science 252*, 1167−1171.
22. Cordingley, M. G., LaFemina, R. L., Callahan, P. L., Condra, J. H., Sardana, V. V., Graham, D. J., Nguyen, T. M., LeGrow, K., Gotlib, L., and Schlabach, A. J. (1990) *Proc. Natl. Acad. Sci. U.S.A. 87*, 8985−8989.
23. Weeks, K. M., Ampe, C., Schultz, S. C., Steitz, T. A., and Crothers, D. M. (1990) *Science 249*, 1281−1285.
24. Wang, S., Huber, P. W., Cui, M., Czarnik, A. W., and Mei, H. Y. (1998) *Biochemistry 37*, 5549−5557.
25. Faber, C., Sticht, H., Schweimer, K., and Rosch, P. (2000) *J. Biol. Chem. 275*, 20660−20666.
26. Puglisi, J. D., Chen, L., Frankel, A. D., and Williamson, J. R. (1993) *Proc. Natl. Acad. Sci. U.S.A. 90*, 3680−3684.
27. Aboul-ela, F., Karn, J., and Varani, G. (1995) *J. Mol. Biol. 253*, 313−332.
28. Litovchick, A., Evdokimov, A. G., and Lapidot, A. (1999) *FEBS Lett. 445*, 73−79.
29. Litovchick, A., Evdokimov, A. G., and Lapidot, A. (2000) *Biochemistry 39*, 2838−2852.
30. Kumagai, I., Takahashi, T., Hamasaki, K., Ueno, A., and Mihara, H. (2000) *Bioorg. Med. Chem. Lett. 10*, 377−379.
31. Hamasaki, K., and Rando, R. R. (1998) *Anal. Biochem. 261*, 183−190.
32. Axelrod, J. H., and Honigman, A. (1999) *AIDS Res. Hum. Retroviruses 15*, 759−767.
33. Zhang, H., Dornadula, G., and Pomerantz, R. J. (1996) *J. Virol. 70*, 2809−2824.
34. Borkow, G., Barnard, J., Nguyen, T. M., Belmonte, A., Wainberg, M. A., and Parniak, M. A. (1997) *J. Virol. 71*, 3023−3030.
35. Delling, U., Roy, S., Sumner-Smith, M., Barnett, R., Reid, L., Rosen, C. A., and Sonenberg, N. (1991) *Proc. Natl. Acad. Sci. U.S.A. 88*, 6234−6238.
36. Calnan, B. J., Biancalana, S., Hudson, D., and Frankel, A. D. (1991) *Genes Dev. 6*, 201−210.
37. Berger, E. A., Murphy, P. M., and Farber, J. M. (1999) *Annu. Rev. Immunol. 17*, 657−700.
38. Kalinkovich, A., Weisman, Z., and Bentwich, Z. (1999) *Immunol. Lett. 68*, 281−287.
39. Frankel, A. D., and Pabo, C. O. (1988) *Cell 55*, 1189−1193.
40. Zagury, D., Lachgar, A., Chams, V., Fall, L. S., Bernard, J., Zagury, J. F., Bizzini, B., Gringeri, A., Santagostino, E., Rappaport, J., Feldman, M., Burny, A., and Gallo, R. C. (1998) *Proc. Natl. Acad. Sci. U.S.A. 95*, 3851−3856.
41. Huq, I., Ping, Y. H., Tamilarasu, N., and Rana, T. M. (1999) *Biochemistry 38*, 5172−5177.
42. Daelemans, D., Schols, D., Witvrouw, M., Pannecouque, C., Hatse, S., van Dooren, S., Hamy, F., Klimkait, T., De Clercq, E., and VanDamme, A. M. (2000) *Mol. Pharmacol. 57*, 116−124.
43. Lapidot, A., Litovchick, A., and Evdokimov, A. G. (2000) Patent 127773, PCT/IL 99/00704, PCT, Int. Publication Number WO 00/39139.
44. Hamy, F., Gelus, N., Zeller, M., Lazdins, J. L., Bailly, C., and Klimkait, T. (2000) *Chem. Biol. 7*, 669−676.
45. Wu, M. X., and Schlossman, S. F. (1997) *Proc. Natl. Acad. Sci. U.S.A. 94*, 13832−13837.
46. Lachgar, A., Bernard, J., Bizzini, B., Astgen, A., Le Coq, H., Fouchard, M., Chams, V., Feldman, M., Burny, A., and Zagury, J. F. (1996) *Biomed. Pharmacother. 50*, 13−18.
47. Ghezzi, S., Noonan, D. M., Aluigi, M. G., Vallanti, G., Cota, M., Benelli, R., Morini, M., Reeves, J. D., Vicenzi, E., Poli, G., and Albini, A. (2000) *Biochem. Biophys. Res. Commun. 270*, 992−996.
48. Cabrera, C., Gutierrez, A., Blanco, J., Barretina, J., Litovchick, A., Lapidot, A., Evdokimov, A. G., Clotet, B., and Este, J. A. (2000) *AIDS Res. Hum. Retroviruses 16*, 627−634.
49. Wang, W. K., Lee, C. N., Dudek, T., Chang, S. Y., Zhao, Y. J., Essex, M., and Lee, T. H. (2000) *AIDS Res. Hum. Retroviruses 16*, 1821−1829.
50. Sakaida, H., Hori, T., Yonezawa, A., Sato, A., Isaka, Y., Yoshie, O., Hattori, T., and Uchiyama, T. (1998) *J. Virol. 72*, 9763−9770.
51. Tugarinov, V., Zvi, A., Levy, R., and Anglister, J. (1999) *Nat. Struct. Biol. 6*, 331−335.
52. Tugarinov, V., Zvi, A., Levy, R., Hayek, Y., Matsushita, S., and Anglister, J. (2000) *Structure 8*, 385−395.
53. Donzella, G. A., Schols, D., Lin, S. W., Este, J. A., Nagashima, K. A., Maddon, P. J., Allaway, G. P., Sakmar, T. P., Henson, G., De Clercq, E., and Moore, J. P. (1998) *Nat. Med. 4*, 72−77.
54. Luedtke, N. W., Baker, T. J., Goodman, M., and Tor, Y. (2000) *J. Am. Chem. Soc. 122*, 12035−12036.
55. Baker, T. J., Luedtke, N. W., Tor, Y., and Goodman, M. (2000) *J. Org. Chem. 65*, 9054−9058.
56. Hamasaki, K., and Ueno, A. (2001) *Bioorg. Med. Chem. Lett. 11*, 591−594.
57. Seewald, M. J., Metzger, A. U., Willbond, D., Rösch, P., and Sticht, H. (1998) *J. Biomol. Struct. Dyn. 16*, 683−692.

BI0108655